JMEPEG (2011) 20:250–256
DOI: 10.1007/s11665-010-9665-6

1059-9495/$19.00

On the Change in Work Hardening Characteristics of Molybdenum Polycrystals Due to Natural Aging

Farooq Bashir, Muhammad Zakria Butt, and Dilawar Ali

(Submitted October 12, 2009; in revised form March 4, 2010)

Strips of 99.95 at.% Mo polycrystals annealed at 700 °C as well as the ones annealed and then aged for 6 months at room temperature were deformed in tension at various strain-rates in the range 2.1×10^{-4} to 4.2×10^{-3} s^{-1} till fracture. It is found that natural aging of the annealed specimens for 6 months leads to 20-30% reduction in the yield stress (YS), 18-22% reduction in the ultimate tensile strength (UTS), and 72-76% reduction in the ductility, i.e. the tensile strain ε_{max} corresponding to UTS, depending on the value of $\dot{\varepsilon}$ in the tensile strain-rate range referred to. Data analysis in terms of the kink-pair nucleation model of flow stress shows that the reduction in YS of the aged Mo specimens is a consequence of lowering of the Peierls energy per interatomic spacing along the length of screw-dislocation segments trapped in the Peierls valleys on the migration of point defects to the dislocation cores during the course of natural aging. The reduction in UTS and ε_{max} is attributed to the variation in the relative contribution of the processes of dislocation multiplication and annihilation together with the reduction in the Peierls stress of the metal.

Keywords aging, ductility, molybdenum, ultimate tensile strength, yield stress

1. Introduction

The phenomenon of natural aging is of paramount importance as far as the performance of engineering materials is concerned. Relaxation processes occur in both nonmetallic (e.g., Ref 1-5) as well as metallic (e.g., Ref 6-13) materials during their prolonged storage at normal conditions and in their service-life time. This leads to subtle microstructural changes in the materials, which effect their performance considerably. For instance, in the case of materials used in electronics and optoelectronic devices, Golovchak et al. (Ref 1) have recently investigated the effect long-term physical aging (~20 years) in vitreous germanium selenides using differential scanning calorimetry methods. They found that the initial glass structure, which seems to be homogenous before aging, moves toward heterogenous one during the long-term natural storage of Ge_xSe_{100-x} ($x < 20$) glasses.

Similarly, in well-annealed solid-solution crystals, which are allowed to age at room temperature for a certain period of time, deviations from random distribution of solute atoms occur, which are manifested by a change in the mechanical response of such crystals (e.g., Ref 6-13). While investigating the concentration dependence of the critical resolved shear stress (CRSS) of copper single crystals alloyed with 1-14 at.% Al at various temperatures in the range 4.2-300 K, Demirskiy et al. (Ref 6) observed that the rate of hardening per solute addition was quite appreciable for the solute concentrations above 7 at.% Al. They opined that "precipitation processes might well develop in specimens held at room temperature," leading to the observed rapid rate of hardening. In a similar investigation carried out with ternary Nb-Hf-W solid-solution crystals, Ruf and Koss (Ref 7) also noticed a rapid rate of hardening at large solute concentrations. They attributed it to the nonrandom distribution of solute atoms rather than the precipitation of a second phase, not detected by transmission electron microscopy techniques. Such effects were also observed by Asif and Butt (Ref 4, 5) in the case of nonmetallic KBr-KCl solid-solution system. To account for the loss of stress-equivalence in concentrated binary solid-solutions, Schwink and Wille (Ref 8) argued that it is the size-misfit factor $\delta = (1/b)\ (db/dc)$, where b is the lattice parameter and c is the solute concentration, which plays a significant role in the formation of clusters of solute atoms in solid-solution crystals. The greater the value of δ, the smaller the critical solute concentration, c_m, to favor solute interactions for the onset of clustering or deviation from a statistical distribution of solute atoms. This view point has recently been confirmed by Butt et al. (Ref 13) in the case of some copper-based alloy systems. They have found a strong systematic correlation between δ and c_m, while other solution-hardening parameters, namely modulus mismatch and electron-to-atom ratio, are of no significance in this regard.

On the other hand, a little work has been done in the case of nominally pure metals. Literature survey shows that hardening of aluminum on natural aging is well established over the years, whereas the effect of natural aging on the stress-relaxation response at a constant strain (Ref 14) and on the strain-rate sensitivity of flow stress (Ref 15) in aluminum has been studied in the recent past. According to Butt and Khwaja (Ref 16), the migration of point defects, e.g., solid and gaseous residual impurity atoms, vacancies in above-equilibrium concentration, etc., to the cores of edge dislocations during natural aging of

Farooq Bashir, Central Research Laboratory, Lahore College for Women University, Lahore 54000, Pakistan; and **Muhammad Zakria Butt** and **Dilawar Ali**, Department of Physics, University of Engineering and Technology, Lahore 54890, Pakistan. Contact e-mail: mzbutt49@yahoo.com.

aluminum, seems to pin the edge dislocations and make their movement rather difficult. This leads to an increase in the yield stress (YS) of naturally aged aluminum crystals compared with that of the unaged ones. The ultimate tensile strength (UTS) of aluminum, however is not effected by natural aging because at rather large strains pinning effects are completely masked (Ref 17). Contrary to it, a reduction in the YS and UTS of molybdenum ($\dot{\varepsilon} = 2.1 \times 10^{-3}\ s^{-1}$) on natural aging for 6 months has recently been reported by Bashir and Butt (Ref 18). However, they observed that for a given stress level at which deformation is interrupted to measure stress relaxation at a constant strain, the relaxation rate was faster in aged specimen of Mo compared with that in unaged ones (Ref 18) as was also reported in the case of Al (Ref 14). Similarly, the reversible change in the flow stress at which strain-rate is lowered by a factor of 10, was also found to increase significantly on natural aging of Mo (Ref 18) like that in Al (Ref 15).

Although the effect of natural aging on the stress relaxation at constant strain and strain-rate sensitivity of flow stress of both Al (fcc) and Mo (bcc) is alike over the entire stress-strain curve, it is in contrast as far as YS and UTS are concerned. The main objective of this study was therefore to investigate quantitatively the cause of reduction in these strength parameters of Mo polycrystals on natural aging. For this purpose, tensile tests were performed at room temperature for a range of strain rates. An analytical expression for the strain-rate dependence of the YS, derived in Ref 19 on the basis of a kink-pair nucleation model of flow stress in crystals with high-intrinsic lattice friction (Ref 20), was used to analyze the YS data. This facilitated the determination of the values of the kink-pair formation energy for the initiation of yielding in just annealed and annealed + naturally aged Mo polycrystals.

2. Theoretical Formulations

Yielding of crystals with high-intrinsic lattice friction occurs through Peierls mechanism in which stress-assisted, thermally-activated, nucleation of a kink-pair in $(a_o/2)<111>$ screw-dislocation segment trapped in a Peierls valley facilitates its forward movement over the Peierls hill to the next Peierls valley, after attainment of the saddle-point configuration. At temperatures below 0.1-0.2 T_{melt}, where diffusional processes are dormant in the crystal, the activation energy (free enthalpy), $W(\tau)$, for the formation of a kink-pair of critical maximum height, nb, for saddle-point configuration is given by (Ref 20)

$$W = 2W_o - 2\alpha_o\tau^{1/2} \qquad \text{(Eq 1)}$$

with the yield criterion

$$W = mkT, \quad m = \ln(\dot{\gamma}_o/\dot{\gamma}) = 25 \pm 2.3 \qquad \text{(Eq 2)}$$

Here $W_o = n(UGb^3)^{1/2}$, $\alpha_o = (1/2)(nb)^{3/2}(Gb^3)^{1/2}$, G is the shear modulus, U is the Peierls energy per interatomic spacing along the screw dislocation, $2W_o$ is the kink-pair formation energy W_{kp} at $\tau = 0$, k is the Boltzmann constant, $\dot{\gamma}$ is the shear rate of the crystal with typical values in the range 10^{-3} to $10^{-5}\ s^{-1}$, and the pre-exponential factor $\dot{\gamma}_o$ is of the order of $10^7\ s^{-1}$.

The critical maximum height, nb, of the kink-pair for saddle-point configuration, where n is a numerical constant and b is the length of the Burgers vector, can be at the most equal to the distance a between two consecutive Peierls valleys. Thus for two consecutive Peierls valleys along $[\bar{1}11]$ direction in bcc crystals, one finds that when $nb = a$, the value of $n = (a/b)$ will be 0.9428, 1.6329, and 2.4945 for (110), (211), and (321) slip planes, respectively.

An analytical expression for the temperature dependence of the CRSS τ for a given strain-rate $\dot{\gamma}$, readily derivable from Eq 1 and 2, is as under (Ref 20):

$$\tau^{1/2} = A - BT \qquad \text{(Eq 3)}$$

where $A = (W_o/\alpha_o) = \tau_o^{1/2}$, $B = (mk/2\alpha_o)$ and $\tau_o = (4U/nb^3)$.

It is evident from Eq 3 that for a given strain rate (i.e., if m is constant), $\tau^{1/2}$ of crystals with high-intrinsic lattice friction decreases linearly with the increase in deformation temperature T.

Similarly, Eq 3 in conjunction with Eq 2 provides an analytical expression for the dependence of the CRSS τ on the shear rate $\dot{\gamma}$ at a constant temperature T at which deformation is carried out (Ref 19):

$$\tau^{1/2} = \tau_o^{1/2} - (kT/2\alpha_o)\ln(\dot{\gamma}_o/\dot{\gamma}) \qquad \text{(Eq 4)}$$

or

$$\tau^{1/2} = C + D\ln\dot{\gamma}, \qquad \text{(Eq 5)}$$

where C and D are positive constants such that

$$C = \tau_o^{1/2} - D\ln\dot{\gamma}_o \qquad \text{(Eq 6)}$$

and

$$D = (kT/2\alpha_o) \qquad \text{(Eq 7)}$$

Equation 5 shows that $\tau^{1/2}$ increases linearly with the increase in $\ln\dot{\gamma}$ such that the slope $[d\tau^{1/2}/d(\ln\dot{\gamma})]$ of the $\tau^{1/2} - \ln\dot{\gamma}$ line fitted to the data at a given temperature T is equal to D. Since D is directly proportional to T (Eq 7), the slope $[d\tau^{1/2}/d(\ln\dot{\gamma})] = D$ (Eq 5) decreases linearly as T is lowered such that $D = 0$ at $T \to 0$ K. Therefore, the value of the constant $C(= \tau_o^{1/2} - D\ln\dot{\gamma}_o)$ should decrease linearly with the rise in temperature T at which deformation is carried out.

3. Experimental Techniques

The polycrystalline molybdenum used was in the form of rolled sheet of 0.13 mm thickness. The main metallic impurities (in at.%) were Fe(0.034), Mn(0.005), Ni(0.005), and Cr(0.004), and the balance 99.952 at.% was Mo. Specimens, 8 cm long and 1 cm wide, were cut from the as-received sheet, and were sealed in a Pyrex glass tube evacuated to 1.3 mPa (10^{-5} torr). These were then annealed at 700 °C for 120 min. The tube was allowed to cool at room temperature before taking out the specimens. The mean grain-diameter of the annealed specimens was found to be 37 μm. The etchant used was 70 mL H_2O + 20 mL H_2O_2 (30%) + 10 mL H_2SO_4. Half of the specimens were subjected to tensile tests at room temperature just after the heat treatment, whereas the remaining ones were allowed to age in air at room temperature for 6 months.

Both annealed and annealed + naturally aged specimens were deformed in tension at four different strain-rates till fracture in a Universal Materials Testing Machine (Model 1195 Instron Ltd., UK) at room temperature. Both ends of the

specimen were held tightly in the wedge-type flat jaws attached to the upper and lower pull rods of the machine such that the gauge length of the specimen was 4 cm. The tensile strain-rates used were $\dot{\varepsilon} = 2.1 \times 10^{-4}$ s^{-1}, 4.2×10^{-4} s^{-1}, 2.1×10^{-3} s^{-1}, and 4.2×10^{-3} s^{-1} corresponding to the cross-head speeds 0.5, 1, 5, and 10 mm/min, respectively. The chart of the load-time recorder was driven at a speed of 50 mm/min, and the full-scale load range used was 2 kN.

4. Results and Discussion

Stress-strain curves were constructed from the load-extension data in the usual manner. Figure 1 depicts some typical engineering stress-strain curves in the plastic region, i.e., excluding the initial linear elastic part, for both unaged and aged 99.952 at.% Mo polycrystal specimens with mean grain-diameter 37 μm, deformed at tensile strain-rates: (a) 2.1×10^{-4} s^{-1}, (b) 4.2×10^{-4} s^{-1}, (c) 2.1×10^{-3} s^{-1}, and (d) 4.2×10^{-3} s^{-1}. The tensile stress σ for plastic strain ε = 0 denotes the value of the tensile YS. It should be noted that strain scale at the top is for unaged specimens and that at the bottom is for aged ones.

4.1 Yield Stress

The stress level on the automatically recorded load-extension curve just above the point where departure from the linearity occurred was taken as the tensile YS. The dependence of tensile YS σ on the tensile strain-rate $\dot{\varepsilon}$ has been illustrated in semi-logarithmic coordinates in Fig. 2. The stars (☆, ★) denote the values of σ for unaged and aged Mo specimens, respectively, deformed at $\dot{\varepsilon}$ in the range 2.1×10^{-4} s^{-1} to 4.2×10^{-3} s^{-1}. Each point denotes an average value of four independent measurements and error

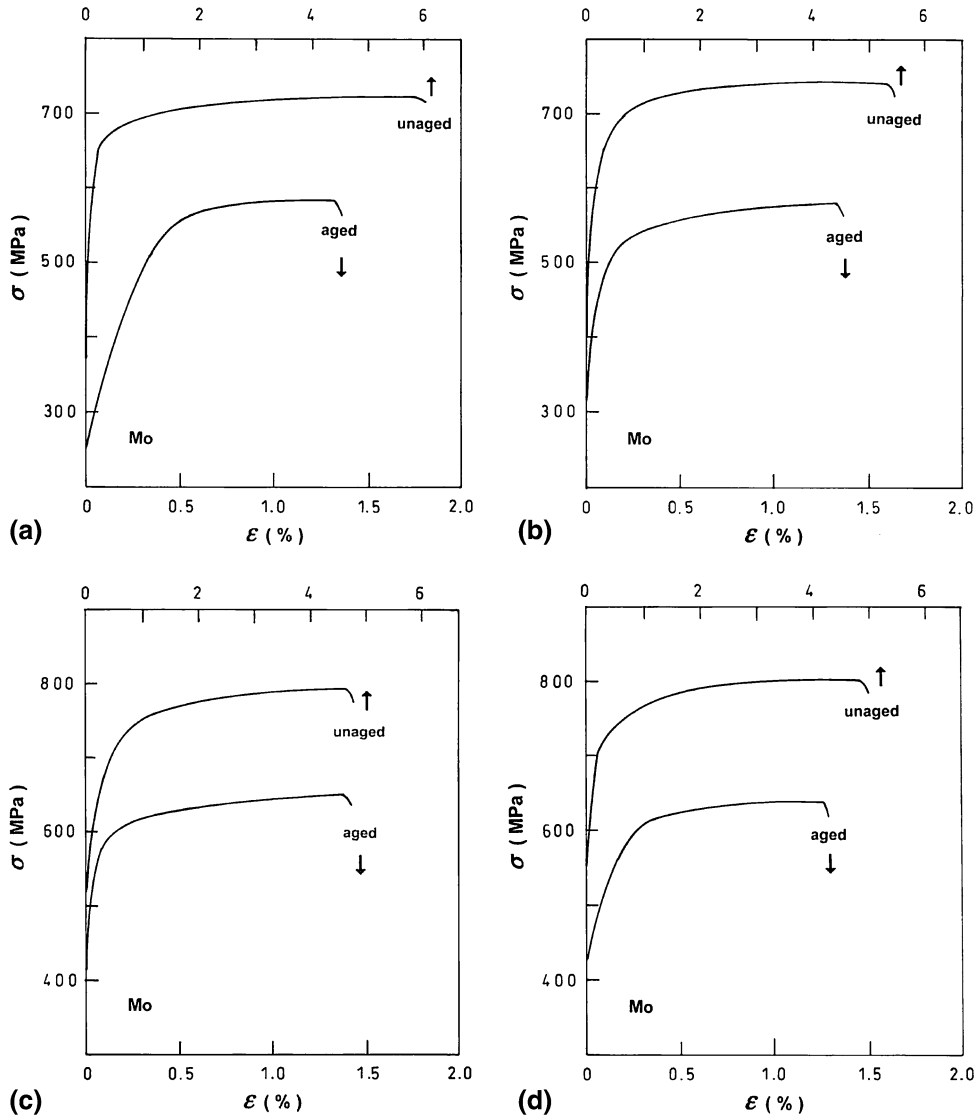

Fig. 1 Some typical stress-strain curves in the plastic region beyond the elastic limit for 700 °C annealed Mo polycrystals (mean grain-diameter = 37 μm) deformed at tensile strain-rates (a) 2.1×10^{-4} s^{-1}, (b) 4.2×10^{-4} s^{-1}, (c) 2.1×10^{-3} s^{-1}, and (d) 4.2×10^{-3} s^{-1}. Strain scale at the top is for unaged specimens and that at the bottom is for aged ones

bars show the range of measured σ values. The straight lines drawn through the data points by least-squares fit are encompassed by the relations:

unaged (☆): $\sigma = 921 + 65.5 \ln \dot{\varepsilon}$ (Eq 8)

aged (★): $\sigma = 760 + 57.9 \ln \dot{\varepsilon}$ (Eq 9)

with the linear correlation coefficient $r = 0.994$ and 0.985, respectively. The values of r close to 1 indicate an excellent linear relationship between σ and $\ln \dot{\varepsilon}$ for each type of specimens. The tensile YS of Mo polycrystals can be seen to decrease on natural aging for 6 months by 20-30% in the strain-range used.

For the purpose of data analysis within the framework of the kink-pair nucleation model outlined in Section 2, we shall now obtain shear values of the YS and the strain rate from the tensile ones using a Taylor factor 1/3, i.e., $\tau = \sigma/3$ and $\dot{\gamma} = 3\dot{\varepsilon}$, and then proceed further as follows. The circles (○, ●) in Fig. 3 denote the values of the square-root of CRSS ($\tau^{1/2}$) of Mo polycrystals as a function of the shear strain-rate $\dot{\gamma}$ in semi-logarithmic coordinates. The empty circles (○) refer to the unaged Mo specimens, while the filled circles (●) appertain to the aged ones. The straight lines drawn through the data points by least-squares fit are represented by the mathematical expressions:

unaged (○): $\tau^{1/2} = 17.6 + 0.88 \ln \dot{\gamma}$ (Eq 10)

aged (●): $\tau^{1/2} = 16.1 + 0.90 \ln \dot{\gamma}$ (Eq 11)

with the linear correlation coefficient $r = 0.994$ and 0.981, respectively. Comparison of Eq 5 and 10 shows that for unaged Mo, $C = 17.6$ MPa$^{1/2}$ and $D = 0.88$ MPa$^{1/2}$. On substituting the value of D in Eq 7, one gets $\alpha_o = 2.33 \times 10^{-24}$ N$^{1/2}$ m^2. Now, on taking $\tau^{1/2} = 12.4$ MPa$^{1/2}$, i.e., the average of four measured values of CRSS$^{1/2}$ denoted by open circles (○) in Fig. 3, and putting it along with $m = (\ln \dot{\gamma}_o/\dot{\gamma}) = 25$, $T = 298$ K, and $\alpha_o = 2.33 \times 10^{-24}$ N$^{1/2}$ m^2 in Eq 4, one gets $\tau_o^{1/2} = 34.4$ MPa$^{1/2}$ or $\tau_o = 1183$ MPa. On using the expression $W_o = \alpha_o \tau_o^{1/2}$, one finds $W_o = 0.501$ eV or $W_{kp} = 1.002$ eV. Also, on putting $C = 17.6$ MPa$^{1/2}$, $D = 0.88$ MPa$^{1/2}$, and $\tau_o^{1/2} = 34.4$ MPa$^{1/2}$ in Eq 6, the value of $\ln \dot{\gamma}_o$ is found to be 19.1, and hence $\dot{\gamma}_o = 1.98 \times 10^8$ s^{-1} or $\dot{\varepsilon} = 6.6 \times 10^7$ s^{-1}, which is of the right order of magnitude, as envisaged in the KPN model.

On using the expressions for the macroscopic parameters $\tau_o = (4U/nb^3)$ and $W_o = n(UGb^3)^{1/2}$, the microscopic parameters n and U of the slip envisaged in the KPN model (Ref 20) are given by the formulae:

$$n^3 = (W_o/Gb^3)^2(4G/\tau_o) \quad \text{(Eq 12)}$$

$$U = (W_o/n)^2(1/Gb^3) \quad \text{(Eq 13)}$$

Similarly, the initial length L_o of the screw-dislocation segment taking part in the unit activation process of yielding at $T \rightarrow 0$ K under the action of applied shear stress, τ_o, and the activation volume, v_o, associated with τ_o, are given by (Ref 20):

$$L_o = b(4Gn/\tau_o)^{1/2} \quad \text{(Eq 14)}$$

$$v_o = (1/4)nL_o b^2 \quad \text{(Eq 15)}$$

Now the various microscopic parameters of slip, i.e., n, U, L_o, and v_o, in unaged Mo polycrystals can be readily obtained from Eq 12 to 15, and are given in Table 1. Similarly, analysis of $\tau^{1/2} - \ln \dot{\gamma}_o$ data pertaining to naturally aged Mo (Fig. 3) yields the value of model parameters τ_o, W_o, n, U, L_o, and v_o, which are also given in Table 1. The value of n for unaged as well as aged Mo polcrystals being close to $a_{(110)} = 0.9428b$ (Fig. 4) points to (110) [$\bar{1}$11] slip system being responsible for yielding at room temperature.

One can readily note from Table 1 that the values of W_o, W_{kp}, and U are reduced on natural aging resulting in lower CRSS τ_o, i.e., softening of Mo polycrystals. This can be accounted for in terms of the migration of point defects, e.g., solid and gaseous residual impurity atoms, vacancies in above-equilibrium concentration, etc., to the cores of screw-dislocations during the course of aging. Consequently, the Peierls field/the cores of

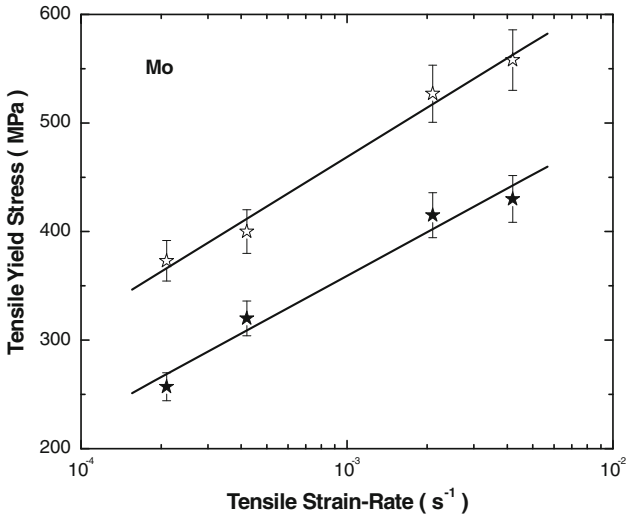

Fig. 2 The tensile yield stress (σ) of 700 °C annealed Mo polycrystals as a function of tensile strain-rate ($\dot{\varepsilon}$) in semi-logarithmic coordinates: (☆) unaged and (★) aged

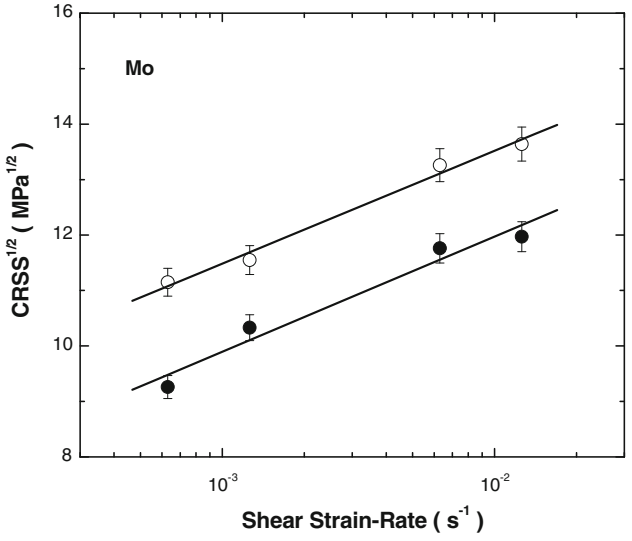

Fig. 3 The square-root of CRSS ($\tau^{1/2}$) of 700 °C annealed Mo polycrystals as a function of shear strain-rate ($\dot{\gamma}$) in semi-logarithmic coordinates: (○) unaged (●) aged

Table 1 Numerical values of various parameters of the KPN model of flow stress in Mo polycrystals

Mo	τ_o, MPa	W_o, eV	W_{kp}, eV	n	U, meV	L_o, b	v_o, b^3	$\dot{\gamma}_o$, s^{-1}	$\dot{\varepsilon}_o$, s^{-1}
Unaged	1183	0.501	1.002	0.75	27.6	18.0	3.4	1.98×10^8	6.6×10^7
Aged	1113	0.476	0.952	0.74	25.6	18.5	3.4	2.04×10^8	6.8×10^7

$G = 12.8 \times 10^4$ MPa, $b = 0.2725$ nm, and $Gb^3 = 16.17$ eV

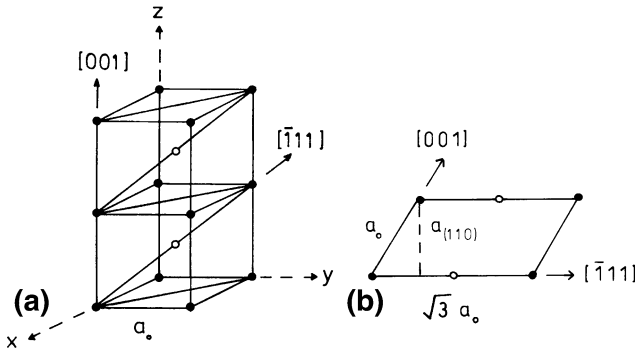

Fig. 4 Schematic representation of (a) the (110) [$\bar{1}$11] slip system and (b) the separation $a_{(110)} = (2/3)^{1/2}a_o = 0.9428b$ between neighboring Pierls valleys along the [$\bar{1}$11] direction in the (110) plane

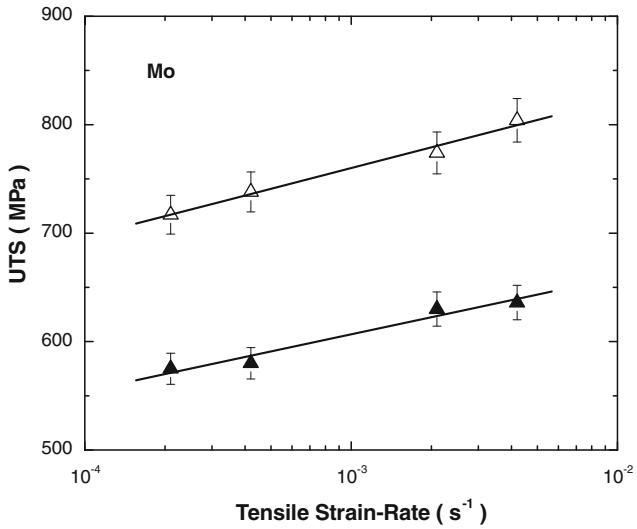

Fig. 5 The UTS of 700 °C annealed Mo polycrystals as a function of tensile strain-rate $\dot{\varepsilon}$ in semi-logarithmic coordinates: (Δ) unaged (▲) aged

screw dislocations are modified leading to lower Peierls energy per interatomic spacing along the length of the screw dislocations trapped in the Peierls valleys, and hence reduction in the YS of naturally aged Mo polycrystals.

As far as the physical explanation of the above is concerned, one can readily conceive that vacancies in above-equilibrium concentration on migration to the cores of screw dislocations trapped in Peierls valleys may produce microscopic kinks in them, and such screw dislocations can escape from the Peierls valleys through the nucleation of macroscopic kink-pairs under a rather lower applied stress as compared to that required for the straight screw dislocations. Thus Peierls energy per interatomic spacing along the length of screw dislocations containing microscopic kinks will be less than that for the straight screw dislocations trapped in Peierls valleys (Table 1). This view point is supported by the investigations of Mitchell et al. (Ref 21), who have demonstrated that cation vacancies, adsorbed on dislocation cores, cause softening in spinel. These vacancies act as catalysts for nucleation of microscopic kink-pairs, whether at two separate vacancies or at a divacancy, which effectively reduces the activation energy.

Concerning the role of interstitial impurity atoms, it is well established that, unlike edge dislocations, the size-misfit interaction is zero to "first order" for screw dislocations, because according to linear elasticity, the stress field of screw dislocations has no hydrostatic component (Ref 22). However, Nabarro (Ref 23) has visualized that in the rate-controlling process of yielding in nominally pure bcc metals or fairly dilute alloys, an impurity atom in the core of a screw dislocation may assist in the nucleation of a kink-pair leading to softening of the crystal. Similarly, Reed-Hill and Kaufman (Ref 24) has found that the basic rate-controlling mechanism of flow stress in commercial purity niobium is not the interaction between interstitial impurity atoms and mobile dislocations; scavenging of interstitials, on the other hand, leads to reduction in flow stress.

4.2 Ultimate Tensile Strength

The stress level corresponding to the peak on the automatically recorded load-extension curve was taken as the UTS. The triangles (Δ, ▲) in Fig 5 denote the values of the UTS of Mo polycrystals as a function of the tensile strain-rate $\dot{\varepsilon}$ in semi-logarithmic coordinates. Each point denotes an average value of four independent measurements and error bars show the range of measured UTS values. The empty triangles (Δ) appertain to the unaged Mo specimens, while the filled triangles (▲) refer to the aged ones. A linear least-squares fit to the data points can be mathematically represented as:

$$\text{unaged } (\Delta): \text{UTS} = 950 + 27.5 \ln \dot{\varepsilon} \qquad \text{(Eq 16)}$$

$$\text{aged } (\blacktriangle): \text{UTS} = 763 + 22.7 \ln \dot{\varepsilon} \qquad \text{(Eq 17)}$$

with the correlation factor $r = 0.993$ and 0.981, respectively.

Referring to Fig 5, one can readily note that the functional form of UTS-$\dot{\varepsilon}$ correlation is the same for both unaged and aged Mo polycrystals. However, the values of the UTS for the aged specimens are 18-22% lower than those for the unaged ones within the tensile strain-rate range studied. This may be associated with the reduction in the Peierls stress on natural aging (Ref 18, 21), which leads to reduction in not only the YS, but also the UTS. Furthermore, the value of UTS for unaged Mo increases by about 12% as the tensile strain-rate $\dot{\varepsilon}$ is increased from 2.1×10^{-4} s^{-1} to 4.2×10^{-3} s^{-1}, whereas the increase in the tensile YS σ of unaged Mo is about 50%. Nearly four times weaker dependence of UTS on $\dot{\varepsilon}$ compared with that of the tensile YS σ is probably due to rather large strains

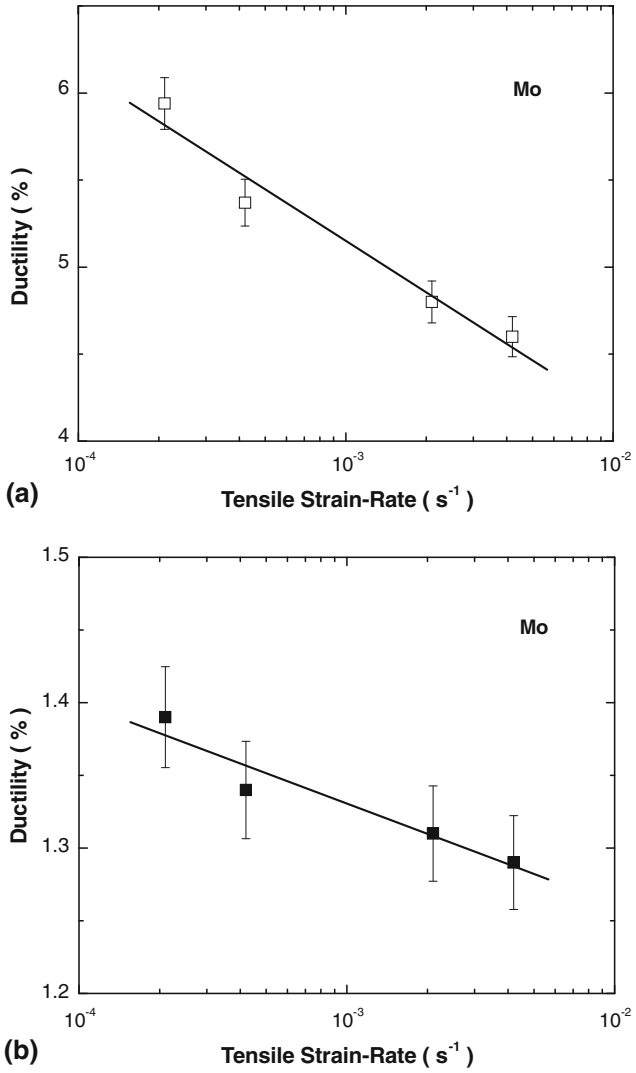

Fig. 6 Relation between ductility ε_{max} and tensile strain-rate $\dot{\varepsilon}$ for 700 °C annealed Mo polycrystals in semi-logarithmic coordinates: (□) unaged (■) aged

involved in the former case (Ref 17). Similar behavior is also observed in the case of aged Mo with the difference that the dependence of UTS on $\dot{\varepsilon}$ is six times weaker as compared to that of tensile yield stress σ.

4.3 Ductility

Referring to Fig. 6, the empty squares (□) and filled squares (■) denote the values of ductility or the tensile strain ε_{max} corresponding to the UTS of unaged and aged Mo polycrystals, respectively, as a function of the tensile strain-rate $\dot{\varepsilon}$ in semi-logarithmic coordinates. Each point denotes an average value of four independent measurements and error bars show the range of measured ε_{max} values. A straight line least-square fit to the data (□) in Fig. 6(a) is encompassed by the relation:

$$\varepsilon_{max} = 2.21 - 0.43 \ln \dot{\varepsilon} \qquad \text{(Eq 18)}$$

with the correlation factor $r = -0.980$. This shows that the ductility ε_{max} of the unaged Mo polycrystal decreases as the tensile strain-rate $\dot{\varepsilon}$ is increased. The reduction in ductility is about 22% as $\dot{\varepsilon}$ is increased from 2.1×10^{-4} s^{-1} to 4.2×10^{-3} s^{-1}.

Similarly, the least-squares fit to the data (■) in Fig. 6(b) can be mathematically represented as

$$\varepsilon_{max} = 1.12 - 0.03 \ln \dot{\varepsilon} \qquad \text{(Eq 19)}$$

with the correlation factor $r = -0.960$. The reduction in the ductility ε_{max} for aged Mo polycrystal is found to be about 7% on increasing $\dot{\varepsilon}$ from 2.1×10^{-4} s^{-1} to 4.2×10^{-3} s^{-1}. Thus the dependence of ε_{max} on $\dot{\varepsilon}$ for aged Mo polycrystal is about three times weaker than that for unaged Mo polycrystal. One can also infer from the data given in Fig. 6 that natural aging of Mo polycrystal for a period of 6 months reduces its ductility by about 72-76% in the tensile strain-rate range referred to above. The shape of the σ-ε curves, however, remains unaffected by the natural aging treatment.

As far as the UTS and the uniform tensile strain ε_{max} prior to the formation of neck during stretching of body-centred cubic (bcc) metals and alloys are concerned, Malygin (Ref 25) has theoretically shown that the magnitude of both the parameters is strongly influenced by the Peierls stress. He considers that in a polycrystalline bcc metal under the conditions of multiple slip, variation of the average dislocation density with the deformation at low and moderate temperatures depends on three factors: (i) the rate of multiplication and accumulation of dislocations interacting with obstacles of nondeformable origin, (ii) the intensity of multiplication of dislocations interacting with forest dislocations, and (iii) the rate of annihilation of the screw segments of dislocation loops. An equilibrium between the processes of dislocation multiplication and annihilation together with the Peierls stress of the metal, determines the tensile strain ε_{max} and the UTS. The observed reduction in the ductility of Mo polycrystals on natural aging may be attributed to the variation in the relative contribution of various structural factors referred to above, and needs a rigorous theoretical treatment in this regard.

5. Summary and Conclusions

One may summarize and conclude from the present investigations as below:

1. The YS of both unaged and aged Mo polycrystals increases with the imposed strain-rate in accord with the analytical expression for the strain-rate dependence of CRSS as predicted by the KPN model of flow stress in crystals with high-intrinsic lattice friction. The same is true for the UTS, but its dependence on the strain-rate is about four times weaker than that of the YS.
2. The YS and the UTS of Mo polycrystals are decreased on natural aging by about 20-30% and 18-22%, respectively, in the tensile strain-rate range 2.1×10^{-4} s^{-1} to 4.2×10^{-3} s^{-1}. The reduction in the YS is due to lowering of the Peierls energy per interatomic spacing along the length of screw-dislocation segments trapped in the Peierls valleys on migration of point defects to the dislocation cores.
3. Natural aging has no effect on the shape of the σ-ε curves of Mo polycrystals, but the ductility ε_{max} decreases by about 72-76% depending on the value of $\dot{\varepsilon}$

in the tensile strain-rate range referred to. The reduction in the ductility may be attributed to the variation in relative contribution of the processes of dislocation multiplication and annihilation together with the reduction in the Peierls stress of the metal.

4. The ductility ε_{max} of unaged Mo polycrystal decreases by about 22% with the increase in the tensile strain-rate $\dot{\varepsilon}$ from 2.1×10^{-4} s^{-1} to 4.2×10^{-3} s^{-1}, whereas the ductility of aged Mo polycrystal is reduced by only 7%.
5. The UTS of unaged and aged Mo polycrystals increases by about 12% and 11%, respectively, as the tensile strain-rate $\dot{\varepsilon}$ is increased from 2.1×10^{-4} s^{-1} to 4.2×10^{-3} s^{-1}, whereas the corresponding increase in the tensile yield stress σ is about 50% and 67%. The strain-rate dependence of UTS is therefore four and six times weaker than that of the tensile YS for unaged and aged Mo polycrystals, respectively.

Acknowledgments

Special thanks are due to the Pakistan Council for Science and Technology, Government of Pakistan, Islamabad, for financial assistance under the Research Productivity Allowance Scheme. We are also indebted to the reviewers for their constructive criticism and valuable suggestions.

References

1. R. Golovchak, A. Kozdras, O. Shpotyuk, S. Kozyuklin, and J.-.M. Saiter, Long-Term Aging Behaviour in Ge-Se Glasses, *J. Mater. Sci.*, 2009, **44**, p 3962–3967
2. S.V. Nemilov, Physical Aging of Silicate Glasses at Room Temperature: The Choice of Quantitative Characteristics of the Process and the Ranking of Glasses by Their Tendency to Aging, *Glass Phys. Chem.*, 2001, **27**, p 214–227
3. P. Boolchand, D.G. Georgiev, and B. Goodman, Discovery of the Intermediate Phase in Chalcogenide Glasses, *J. Optoelectron. Adv. Mater.*, 2001, **3**, p 703–720
4. A. Asif and M.Z. Butt, Analysis of Observations on Solid-Solution Hardening in KBr-KCl Single Crystals, *J. Mater. Sci.*, 2007, **42**, p 2862–2866
5. A. Asif and M.Z. Butt, Analysis of Temperature and Concentration Dependences of Flow Stress in KCl-KBr Single Crystals with Special Reference to the Nature of Solute Distribution, *Phil. Mag.*, 2007, **87**, p 1811–1820
6. V.V. Demirskiy, S.N. Komnik, and V.I. Startsev, Work Hardening of Single Crystals of Copper-Aluminum α Solid Solutions in the Range 4.2-300 K, *Phys. Met. Metall.*, 1979, **46**, p 51–158
7. R. Ruf and D. Koss, Solid-Solution Hardening of the Ternary System Nb-Hf-W, *Phil. Mag.*, 1974, **30**, p 1319–1326
8. C. Schwink and T. Wille, On the Concentration Dependence of Stress Equivalence in Solid Solution Hardening, *Scripta Metall.*, 1980, **14**, p 1093–1100
9. A. Varschavsky and E. Donoso, A Calorimetric Investigation on the Kinetics of Solute Segregation to Partial Dislocations in Cu-3.34 at.%Sn, *Mater. Sci. Eng. A*, 1998, **251**, p 208–215
10. R.C. Picu, G. Vinczc, J.J. Gracio, and F. Barlat, Effect of Solute Distribution on the Strain Rate Sensitivity of Solid Solutions, *Scripta Mater.*, 2006, **54**, p 71–75
11. H. Sieurin, J. Zander, and R. Sandstrom, Modelling Solid Solution Hardening in Stainless Steels, *Mater Sci. Eng. A*, 2006, **415**, p 66–71
12. M.Z. Butt and F. Aziz, Effect of Heterogeneous Solute Distribution on the Anomalous Theremo-Mechnical Response of Cu-Ni Alloy Single Crystals Below 50 K, *Phil. Mag. Lett.*, 2007, **87**, p 915–922
13. M.Z. Butt, M. Noshi, and F. Bashir, Onset of Local Ordering in Some Copper-Based Alloys: Critical Solute Concentration Vis-à-Vis Various Solution Hardening Parameters, *Cent. Europ. J. Phys.*, 2008, **6**, p 834–842
14. M.Z. Butt, M. Zubair, and I. Ul-Haq, A Comparative Study of the Stress Relaxation in Aged and Un-Aged High-Purity Aluminium Polycrystals, *J. Mater. Sci.*, 2000, **35**, p 6139–6144
15. M.Z. Butt, A.Q. Jakhar, and H. Aslam, Effect of Natural Aging on the Strain-Rate Sensitivity of Flow Stress in High-Purity Aluminium Polycrystals, *Phys. Stat. Sol. (a)*, 1999, **176**, p 877–884
16. M.Z. Butt and F.A. Khwaja, Effect of Aging on the Strength of High-Purity Aluminium, *J. Nat. Sci. Math.*, 1995, **35**, p 1–4
17. M.Z. Butt and P. Feltham, Work Hardening of Polycrystalline Copper and Alpha-Brasses, *Metal Sci.*, 1984, **13**, p 123–126
18. F. Bashir and M.Z. Butt, Effect of Natural Aging on the Mechanical Properties of Molybdenum Polycrystals, *J. Mater. Sci.*, 2007, **42**, p 7801–7805
19. M.Z. Butt, M. Khaleeq-ur-Rahman, and D. Ali, On the Strain-Rate Dependence of Flow Stress in Crystals with High Intrinsic Lattice Friction, *J. Phy. D: Appl. Phys.*, 2009, **42**, p 035405
20. M.Z. Butt, Kinetics of Flow Stress in Crystals with High Intrinsic Lattice Friction, *Phil. Mag.*, 2007, **87**, p 3595–3614
21. T.E. Mitchell, P. Peralta, and J.P. Hirth, Deformation by a Kink Mechanism in High Temperature Materials, *Acta Mater.*, 1999, **47**, p 3687–3694
22. R.L. Fleischer, Substitutional Solution Hardening, *Acta Metall.*, 1963, **11**, p 203–209
23. F.R.N. Nabarro, Solution Hardening, *Dislocations and Properties of Real Materials*, M.H. Loretto, Ed., The Institute of Metals, London, 1985, p 152–169
24. R.E. Reed-Hill and M.J. Kaufman, On Evaluating the Flow Stress in Niobium of Commercial Purity, *Acta Metall. Mater.*, 1995, **43**, p 1731–1739
25. G.A. Malygin, Structure Factors that Influence the Stability of Plastic Strain of bcc Metals Under Tensile Load, *Phys. Solid State*, 2005, **47**, p 896–902